

Koichi YONEMOTO⁺Kawasaki Heavy Industries, Ltd.
Aircraft Engineering Division
Kakamigahara, Gifu, Japan

Abstract

An approach which modifies a subsonic doublet lattice method was proposed in the calculation of transonic unsteady aerodynamics. In this approach, phase shifts as well as amplitudes of pressure load distributions on a wing were modified in use of the doublet lattice method. This method was developed as an approximate, but practical technique for calculating the transonic flutter boundary on a parametric wing design stage of an aircraft.

With the aim of obtaining data for verification of the present method, model flutter experiment was performed on an energy efficient supercritical transport wing with an aspect ratio of 10.5 and with a swept angle of 18 degrees. The measured flutter boundary exhibited a sharp drop for the narrow Mach number region around 0.8 and was 20% lower in dynamic pressure than that by the subsonic lifting surface theory.

Flutter characteristics predicted by the present method were compared with experimental results, and it was found that their shape in a "transonic dip" agrees well with that obtained from the experiments.

1. Introduction

Recent transport aircraft design tends to employ a higher aspect ratio and lower swept angle wing with newly developed supercritical airfoil sections for the purpose of energy efficiency in the transonic speed range.

From the structural viewpoint, such a high aspect ratio wing becomes very critical on aeroelastic phenomena, which are represented by flutter and aileron reversal, etc. More importantly, it is pointed out that the introduction of the supercritical airfoils can deteriorate wing flutter characteristics in the transonic range. As demonstrated in a couple of supercritical wing wind tunnel flutter experiments by Farmer and Hanson⁽¹⁾ and others^{(2), (3)}, there exists a so-called "transonic dip" of steep declining of flutter speeds, and the phenomena cannot be explained by the linear lifting surface theory. This problem is very complicated, but urgent. Aircraft engineers must pay enough attention to it even on a preliminary design stage.

^{*}This investigation was carried out under contract with JADC (Japan Aircraft Development Corporation) in conjunction with the development of YXX (forthcoming transport aircraft) project.

⁺ Research Engineer, Aerodynamic Engineering Section

Although sophisticated numerical methods for the unsteady transonic flow have been making remarkable progresses, an appropriate method as a design tool has not yet been available. These methods are now being in verification and still consume much computation time, while the aircraft engineers need quick solutions to apply flutter calculation results to wing structural design.

Several approximate approaches have, on the other hand, been proposed for predicting the transonic flutter speed boundary. It is shown that well known Yates' modified strip analysis can be applied to this problem.⁽⁴⁾ This method modifies steady state spanwise distribution of the section lift curve slope and aerodynamic center by using wind tunnel data. Another approach was derived by Garner⁽⁵⁾, where he simulated not only spanwise lift but also chordwise pressure distributions by modifying kernel functions of two dimensional subsonic lifting surface theory according to experimental or theoretical steady state pressure distributions. The simulated aerodynamic forces were in good agreement with experimental results, but its application to flutter calculation has not yet been seen.

This paper proposes an approximate approach for transonic flutter calculations, which can be applied to the preliminary and parametric wing design. The present method is an extended approach of Yates and Garner and takes account of not only spanwise and chordwise pressure amplitude distributions but also phase shifts of aerodynamic forces caused by shock wave motions. The pressure amplitude correction data can be obtained from static measurements or steady state calculations of the surface pressure. Concerning the phase shifts of aerodynamic forces relative to airfoil motions, an empirical rule was formulated in the present analysis, which was referred to Tijdeman's close experimental observations of the unsteady transonic flow.⁽⁶⁾

2. Transonic Flutter Analysis

2.1 Background of Transonic Flutter Phenomena

The transonic flow regime is one where subsonic and supersonic flows are mixed, and the flow pattern around a wing is complicated because of the existence of shock wave motions on its surface. Once a shock wave appears, the unsteady pressure distribution differs absolutely from what is predicted by the subsonic lifting surface theory. Recent advanced numerical calculation results^{(7)~(9)} and wind tunnel experiments^{(10), (11)} gradually reveal the characteristics of shock wave motions to us. Based on the wind tunnel test results, for example, which were conducted by Tijdeman at NLR in Netherlands, some typical characteristics of unsteady transonic pressure distributions around two dimensional oscillating airfoils can be observed and described as follows,

- (1) Shock wave motions cause remarkable surface pressure amplitude peak.
- (2) The pressure phase distribution relative to airfoil oscillations lags in front of the shock wave and leads ahead beyond it.

These effects are considered to play important roles on the transonic dip mechanism of the flutter boundaries. ⁽⁷⁾

2.2 Correction for Including transonic Effects

The correction techniques to incorporate transonic effects are outlined in this paragraph. The corrections are done by introducing transonic pressure amplitude and phase shift modifications into the subsonic doublet lattice method.

Pressure Amplitude Distribution

Tijdeman's experimental study implies that the amplitude of unsteady pressure distributions associated with shock waves shows the shape similar to those observed in the quasi-steady transonic load. In the present method, the unsteady pressure amplitude with transonic effect for each aerodynamic box is obtained by multiplying unsteady subsonic pressure amplitude by the correction factor. This factor is the ratio of the three dimensional quasi-steady transonic to subsonic load at each aerodynamic box.

Thus

$$|\Delta C_{p,u}|_{\text{transonic}} = |\Delta C_{p,u}|_{\text{subsonic DLM}} \cdot \frac{|\Delta C_{p,\alpha,qs}|_{\text{transonic}}}{|\Delta C_{p,\alpha,qs}|_{\text{subsonic DLM}}} \quad (1)$$

Phase Shift of Pressure Distribution

The effect of the transonic flow on the phase shift of the pressure distribution is included in this method by assuming chordwise phase shift differences of pressure distributions between unsteady subsonic and transonic flows. Figure 1 displays the proposed phase shift differences which have a sharp 180 degree jump at the shock position and vary linearly from the shock position to the leading and trailing edges and become zero at both edges. Figure 2 shows a typical chordwise pattern of transonic and subsonic pressure phase shifts.

To obtain the shift difference value ϕ_s at the shock position, an empirical equation is introduced in the present analysis as follows.

$$\phi_s = \bar{\phi}_k \cdot x_s^* [1 - \text{EXP}(-S \cdot M_\infty \cdot k^T)] \quad (2)$$

$$S = 20.1$$

$$T = 1.5$$

where the $\bar{\phi}_k$ is derived from the next equation.

$$\bar{\phi}_k = 2 \frac{C}{C_{ref}} \cdot M_\infty \cdot \int_{x_s^*}^1 \frac{1}{1 - [R(M - M_\infty) + M_\infty]} \cdot \left(\frac{a_\infty}{a}\right) dx^* \quad (3)$$

- a : local speed of sound
- a_∞ : free stream speed of sound
- c : local chord length
- C_{ref} : reference chord length
- k : reduced frequency
- M : local Mach number
- M_∞ : free stream Mach number
- R : relaxation factor = 0.7 ⁽⁸⁾
- U_∞ : free stream velocity
- x : chordwise coordinate
- x^* : non-dimensional coordinate = x/c

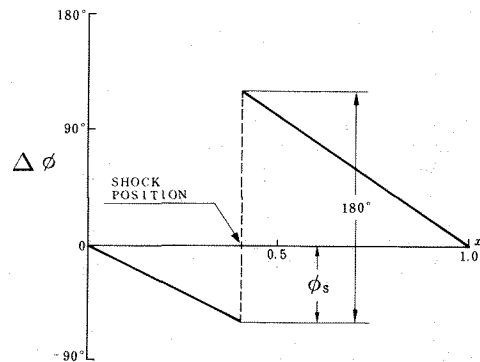


Figure 1. Phase Shift Difference of Pressure Distribution between Transonic and Subsonic Flows

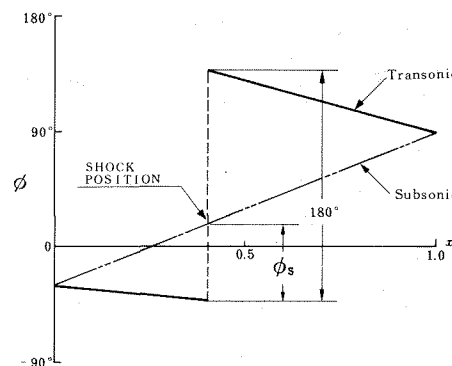


Figure 2. Corrected Phase Distribution of Pitching Oscillation

This empirical rule is the outcome based on the following considerations.

- (1) The ϕ_s increases linearly with the reduced frequency k, when the k is relatively small. Tijdeman has measured the lag time of shock wave motion relative to the airfoil oscillation and pointed out that the time increases linearly with respect to the oscillating frequency. Since the phase shift ϕ_s is caused by the time lag of the shock wave motion, it can be assumed to be also linear with respect to the reduced frequency.

(2) But as was mentioned and summarized by Ashley⁽¹²⁾ and Nixon⁽¹³⁾, the ϕ_s approaches a certain ceiling value when the k is large, referring to several experimental and analytical results. In this paper the ceiling value is hypothesized as the product of $\bar{\phi}_k$ multiplied by x_s^* . The $\bar{\phi}_k$ is derived from the equation which Tijdeman has expressed for the 'Kutta Wave' lag time Δt in his paper.⁽⁶⁾

Namely

$$\Delta t = - \int_{x_s^*}^{x^*} \frac{dx}{c \{ 1 - [R(M - M_\infty) + M_\infty] \cdot a} \quad (4)$$

and

$$\phi_k = \omega \cdot \Delta t = \bar{\phi}_k \cdot k \quad (5)$$

ω : natural circular frequency

The x_s^* is the non-dimensional chordwise shock location, which plays a role of weighting function expressing the length of the supersonic region. It means that the influence of the pressure phase shift of a shock wave near the leading edge is small. This ceiling value has about the value that Ashley referred to.

- (3) The unknown values S and T were chosen for the empirical equation to correspond with the experimental results obtained by Tijdeman, as shown in Figure 3. Figure 4 indicates the phase shift curve with respect to the reduced frequency k for various free stream Mach numbers.
- (4) Since the above phase shift is considered for the surface pressure distribution, it is assumed that the contribution to the load is half.

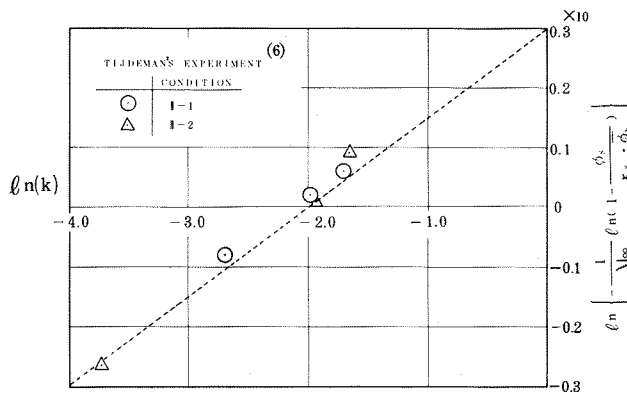


Figure 3. Estimation of Parameters S and T in Empirical Equation of Phase Shifts ϕ_s

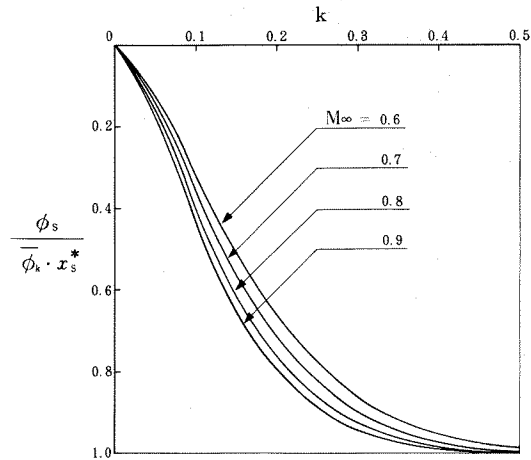


Figure 4. Phase Shift Curves Relative to Reduced Frequency for Various Mach Numbers

2.3 Calculation procedure

At the outset one performs steady state transonic flow calculations around a wing or obtains the pressure distributions from wind tunnel results, if available, and derives the quasi-steady pressure distributions from them.

In the present analysis, FLO22⁽¹⁴⁾ code was employed for obtaining three dimensional steady state transonic pressure distributions around the wing.

According to the method mentioned in the previous paragraph, the correction factors for the load distributions can be expressed in the matrix form of complex numbers.

The calculation is performed by using the module utility of the aeroelastic analysis version of NASTRAN program. The flutter equation is finally solved by K, KE or PK method in U-g procedure. The flow chart is shown in Figure 5.

3. Wind Tunnel Results and Comparison with Analysis

The transonic wind tunnel flutter experiment was conducted to obtain experimental data for the evaluation of the present correction method.

3.1 Wind Tunnel Flutter Experiment

Wind Tunnel Model

The wing flutter model is designed as a 1/45 size transport wing with an aspect ratio of 10.5 and an 18 degree swept angle. The model is a semi-span version and is cantilever-mounted in the wind tunnel wall. Descriptions of the geometry are shown in Figure 6, together with airfoil sections. This wing model employs so-called "rear loading type" of supercritical wing sections, of which the airfoil thickness is about 16% at the root and 12% at the tip.

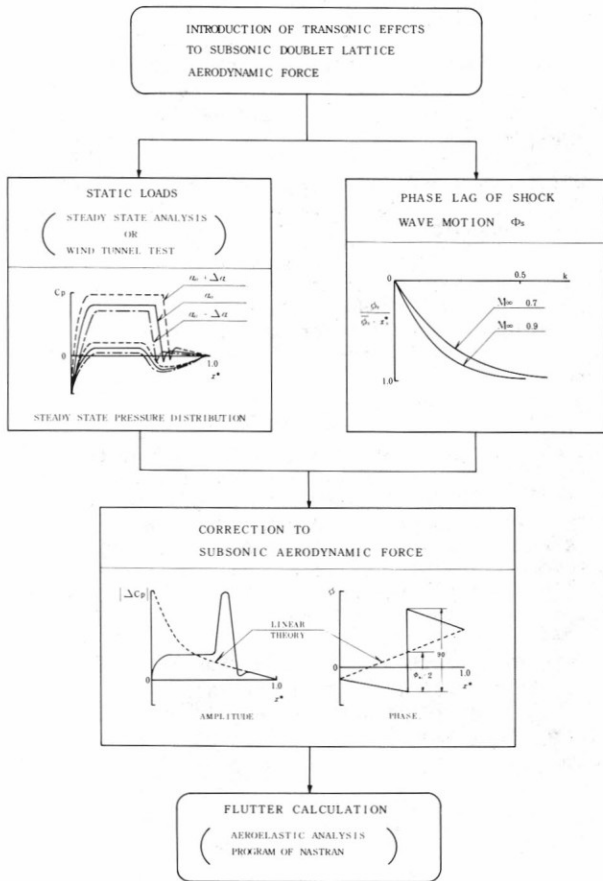
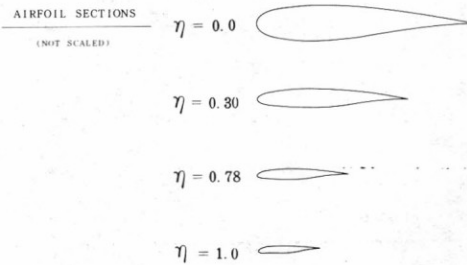
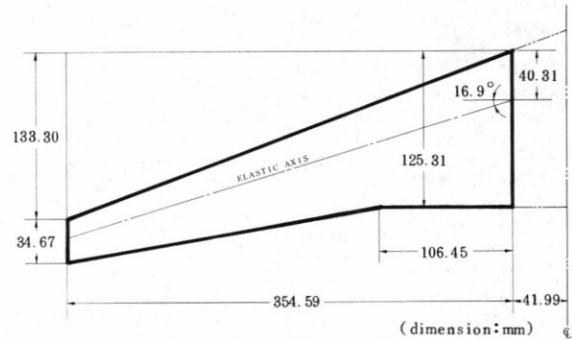


Figure 5. Flow Chart of Flutter Calculation with Transonic Effects



ASPECT RATIO AR	10.5 (10.0)
SWEPT ANGLE $AC/4$	18
TAPER RATIO λ	0.3 (0.324)
MODEL SCALE	1:45

() : EXPOSED

Figure 6. Geometry of Flutter Model

The model is constructed from an aluminum integral structure of a spar, ribs, and webs, and silk covered foamed plastics to provide aerodynamic contours (Figure 7). Structural properties, such as spanwise bending and torsional stiffness are simulated by the spar and validated through stiffness and vibration tests. Comparisons of measured with analytical vibration characteristics are summarized in Table 1 and Figure 8, which show good agreement between them.

Experimental Procedure

Experimental studies were conducted in the 0.6m by 0.6m blow-down transonic flutter wind tunnel at the National Aerospace Laboratory in Tokyo, Japan. During the flutter experiment, the tunnel was operated in the manner of sweeping stagnation pressure with a constant Mach number. The experiment covered a Mach number range from about 0.65 to 0.95. Motion response measured through the use of strain gage bridges on the model was monitored on strip charts and a real-time Fast Fourier Transform analyzer. Flutter boundaries and frequencies were derived from the filtered data of the response which was stored on a data recorder. A TV camera was also used for monitoring a continuous visual record of the model behavior.

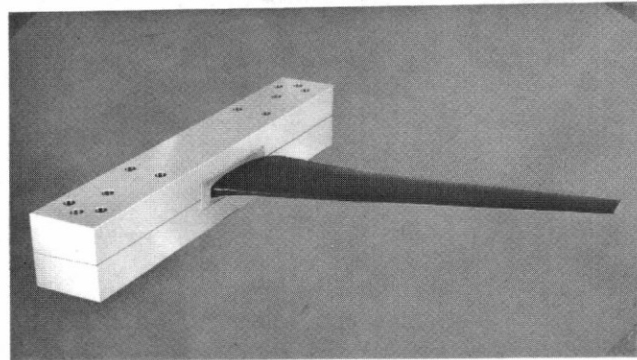


Figure 7. Flutter Model Mounted in a Supporting Block

Experimental Results

Table 1. Summary of Natural Vibration Characteristics of Flutter Model

MODE	EXPERIMENT		ANALYSIS	
	NATURAL FREQ. (Hz)	STRUCTURAL DAMPING (g)	NATURAL FREQ. (Hz)	GENERALIZED MASS (kgf-S ² /m)
1	61.9	0.0140	60.7	3.551×10^{-5}
2	206.1	0.0130	200.6	3.423×10^{-6}
3	413.2	0.0156	429.4	4.580×10^{-7}
4	458.7	0.0146	448.2	1.190×10^{-6}
5	705.7	0.0296	702.4	3.281×10^{-7}
6	794.0	—	816.9	5.819×10^{-7}
7	959.0	—	952.4	1.766×10^{-7}

One of the typical flutter experimental results was shown in Figure 9. Measured flutter dynamic pressures were plotted against Mach numbers in the lower part of this figure, and corresponding flutter frequencies in its upper part. This figure shows a precise picture of the transonic dip which has been known as a phenomenon peculiar to the transonic flutter of the supercritical wing. The dip of the flutter boundary occurred in the relatively narrow Mach number region between 0.75 and 0.85. At Mach=0.94, the model was stabilized considerably and no flutter was recorded within the tunnel operating range of the dynamic pressure.

At the bottom of the dip, a low damping unstable motion was observed as indicated in references (1), (15). This situation was illustrated in Figure 10, where examples of time history response of the model motion obtained from the output signal of a strain gage bridge were presented at several experimental points. It can be seen that the unstable motion never happens to become explosive flutter at this bottom.

In this flutter experiment, the incidence angle at the root of wing was set at $\alpha_r=0^\circ$ and 2° , but significant differences of measured flutter characteristics between them were not detected.

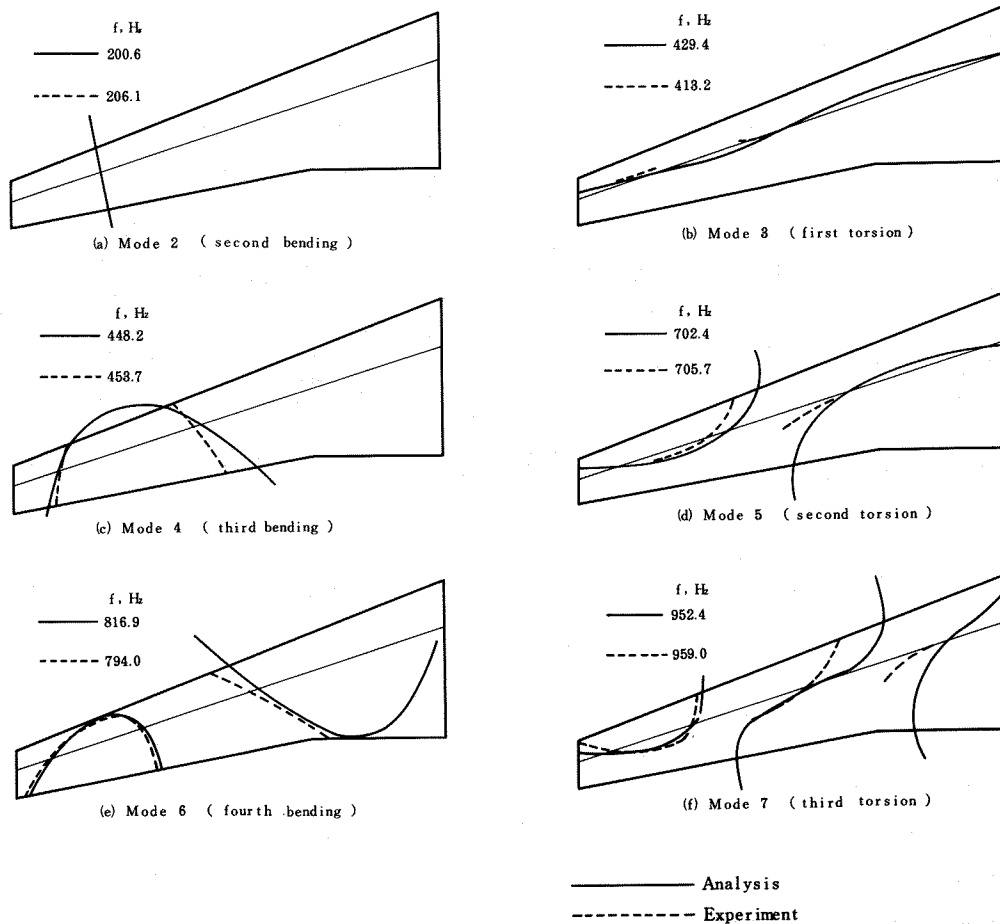


Figure 8. Comparison of Analytical and Experimental Nodal Lines of Natural Vibration Mode

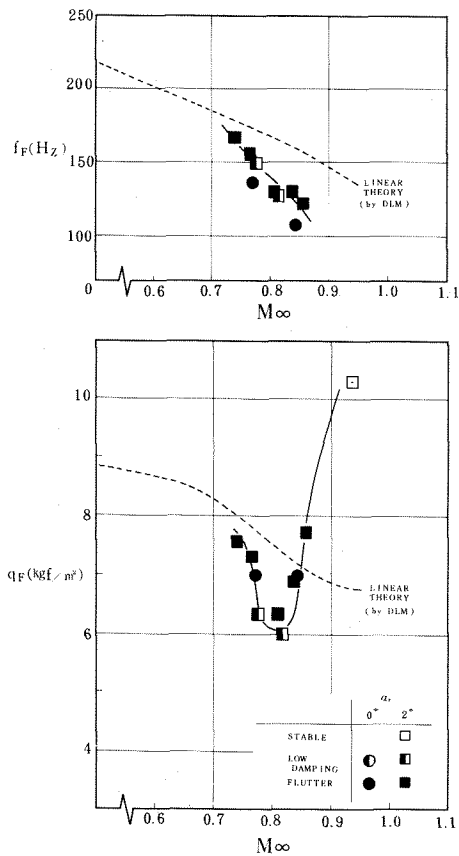


Figure 9. Measured Flutter Characteristics

3.2 Analytical Results and Correlation With Experimental Data

Prior to flutter analyses, steady state transonic aerodynamics are calculated using FLO22. Figure 11(a) presents examples of calculated steady state transonic pressure distributions at Mach=0.8 and $\alpha_r=2^\circ$. Corresponding quasi-steady pressure distributions are shown in Figure 11(b). The righthand side figure in Figure 11(b) is a quasi-steady load distribution for each aerodynamic box and is utilized for deriving the pressure amplitude correction factor in Eq.(1). Examples of modified unsteady load distributions are illustrated in Figure 12, where wing flutter model oscillates in the first torsional mode at Mach=0.8, $\alpha_r=2^\circ$, and $k=0.2$. The unsteady load distributions with both amplitude and phase corrections are almost perfectly different from those of the subsonic doublet lattice method. In addition to pressure amplitude and phase correction, the effect of the boundary layer thickness on the quasi-steady load distribution is also included when steady state transonic aerodynamics are calculated using FLO22.

Figure 13 showed the analytically and experimentally derived flutter characteristics of the wing model. Three analytical flutter boundaries are compared in order to specify each correction effect on the transonic dip. It can be seen in Figure 13 that the results of the present analyses predict the transonic dip, which cannot be estimated by using the linear subsonic doublet lattice method. The flutter boundary obtained without the phase correction leads to higher flutter dynamic pressure at Mach=0.75 than do the boundaries with the phase correction. It is clear that the phase

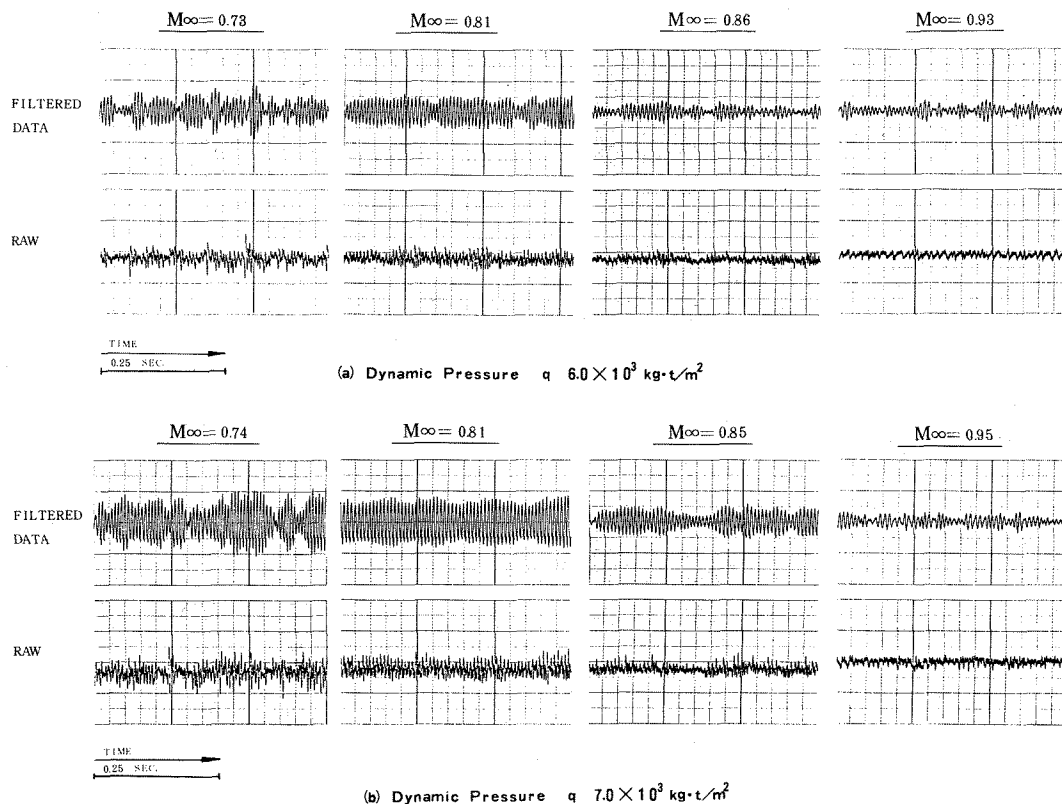
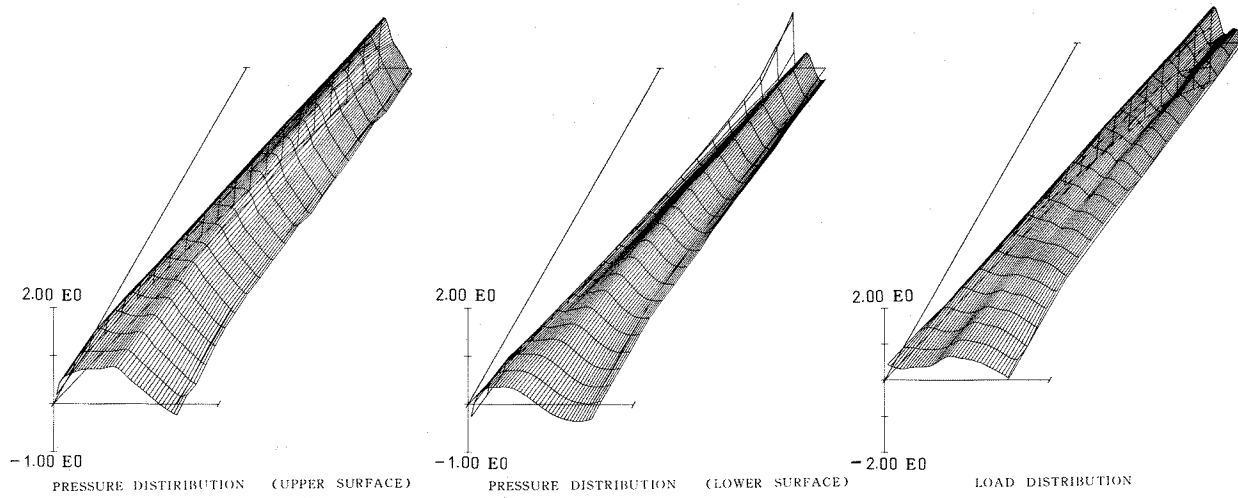
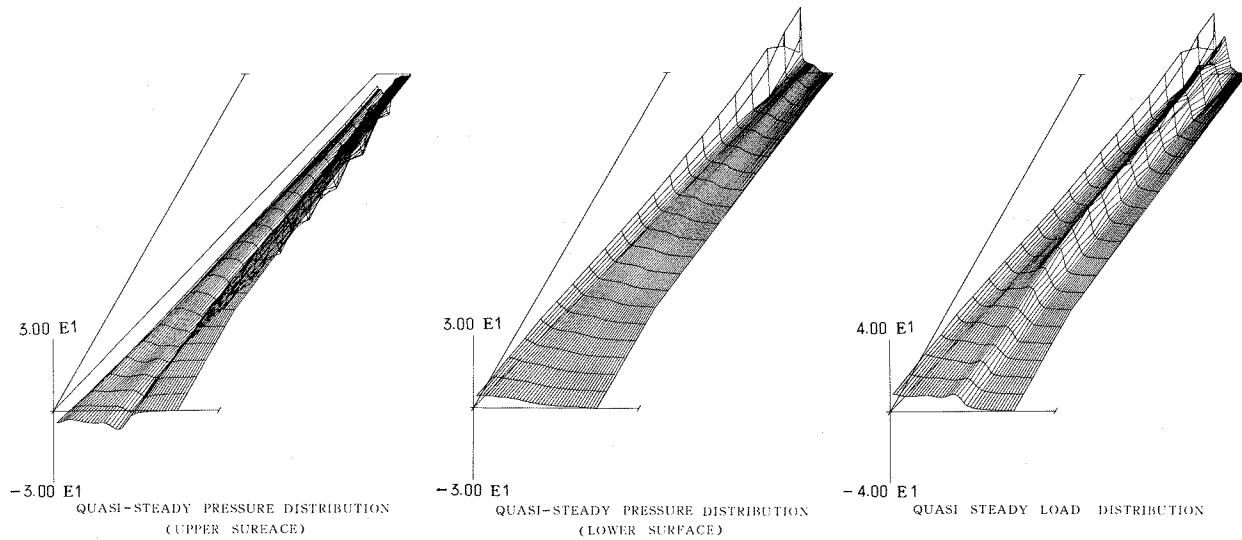


Figure 10. Example of Time Histories of Dynamic Responses of Flutter Model



(a) Pressure and Load Distributions



(b) Quasi - Steady Pressure and Load Distributions

Figure 11. Steady State and Quasi-Steady Pressure Distributions Obtained from FLO22 ($M_\infty=0.8$, $\alpha_r=2^\circ$)

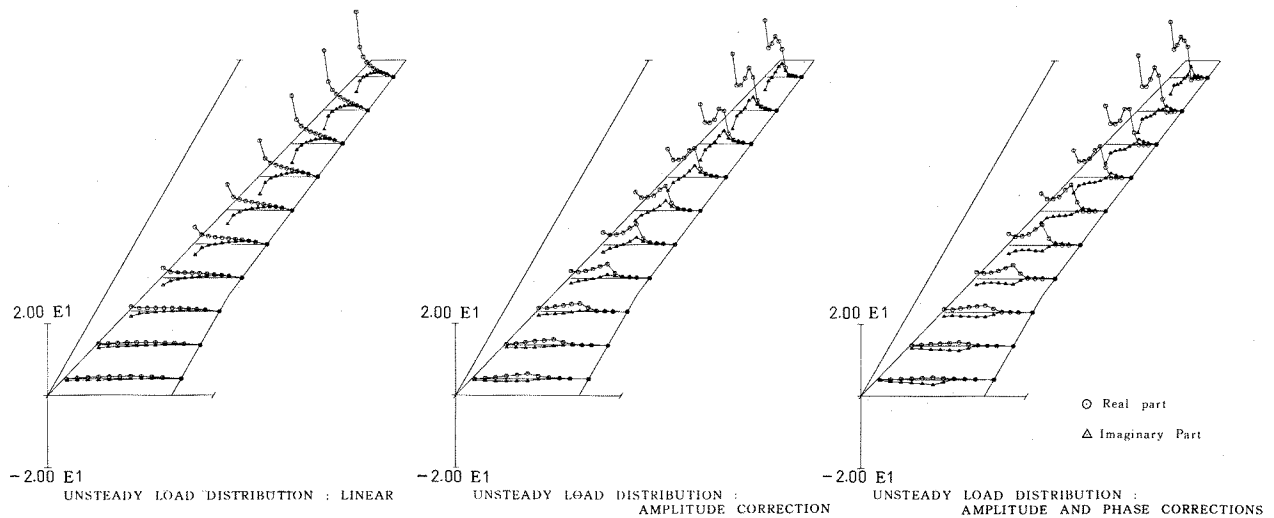


Figure 12. Unsteady Transonic Load Distributions of Oscillating Flutter Model in the First Torsional Mode ($M_\infty=0.8$, $\alpha_r=2^\circ$, $k=0.2$)

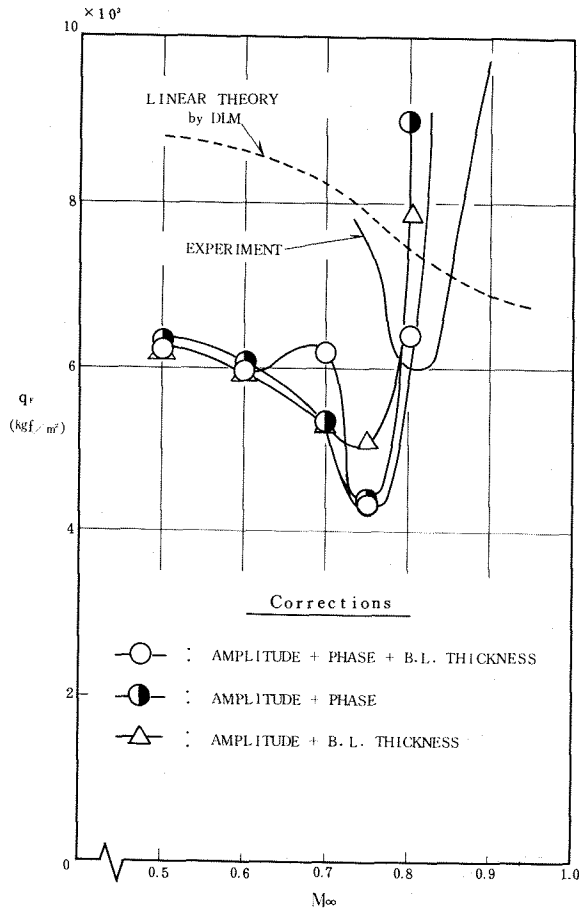
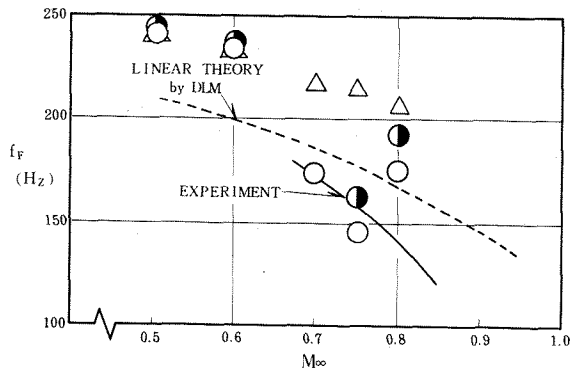


Figure 13. Flutter Boundaries Predicted by the Present Method in Comparison with Experiment

correction of pressure distribution have some relation to the depth of the transonic dip. At Mach=0.8, the system is stabilized significantly. This stabilization is mainly attributed to the effect of transonic pressure amplitude distribution, whose peak shifts to the downstream direction on the wing surface for higher Mach number region.

The analytical-experimental correlations in the shape of the transonic dip show reasonable agreement. Especially the width and depth of the dip are well-correlated. The flutter bounda-

ries themselves, on the other hand, show some discrepancy quantitatively in Figure 13. Incidentally, there appears some analytical difference between the results of the doublet lattice method and the present analyses even at Mach=0.6, where the flow around the oscillating wing is subsonic. The reason for the difference of the flutter dynamic pressures around the transonic dip may come from the same reason for the difference at Mach=0.6. This problem needs further investigation. As for the Mach number which gives the bottom of the transonic dip, the analytical Mach number is lower by 0.05 than the experimental one. Earlier discussion indicates that the phase correction seems to have a major effect on the shape of the analytical transonic dip. This Mach number difference between analysis and experiment possibly comes from the way of phase correction in the analysis.

Figure 14 presents analytical U-g and U-f curves of the critical mode for various Mach numbers. Although the low damping unstable motion was experimentally observed around the bottom of the transonic dip, this tendency is not recognized in the U-g curve for Mach=0.75.

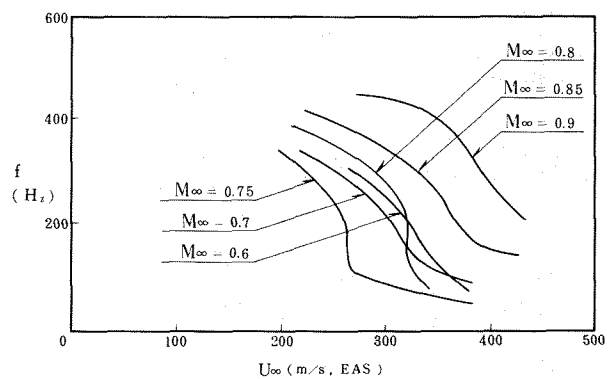
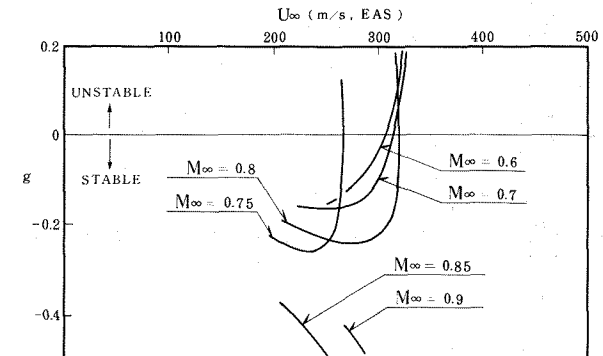


Figure 14. U-g Curves Calculated by the Present Method (First Torsional Mode Branch)

4. Concluding Remarks

A study of the proposed approximate method and the results of flutter experiments lead to the following conclusions.

- (1) The introduction of correction of pressure phase shift distribution as well as amplitude gives better correlation between analysis and experiment than that with the amplitude correction only.
- (2) Better correlation with experiment in the shape of the transonic dip is obtained when the correction of phase shifts of pressure load distributions is included.
- (3) In the transonic flutter experiment, the complete shape of the transonic dip was determined successfully, and the low damping unstable motion was observed around the bottom of the transonic dip.
- (4) Further study to improve the empirical rule for phase shifts will be required in order to obtain better quantitative correlation.

Acknowledgements

This investigation was performed in the program of developing the next short range transport aircraft, namely YXX project which is now being planned by JADC (Japan Aircraft Development Corporation). The author thank Dr. K.Hiraoka of JADC and Dr. K.Isogai of Aeroelastic Research Section of Airframe Division of NAL (National Aerospace Laboratory in Tokyo, Japan) for their suggestions and encouragements in this work.

References

1. Farmer, M.G. and Hanson P.W.: "Comparison of Supercritical and Conventional Wing Flutter Characteristics," Proceedings of AIAA/ASME/SAE 17th Structure, Structural Dynamics and Material Conference, May 1976.
2. Houwink, R., Kraan, A.N. and Zwaan, R.J.: "Wind Tunnel Study of the Flutter Characteristics of a Supercritical Wing," Journal of Aircraft, Vol.19, No.5, May 1981.
3. Person, A.J., Horsten, J.J. and Meijer, J.J.: "On Measuring Transonic Dip in the Flutter Boundaries of a Supercritical Wing in the Wind Tunnel," AIAA Paper No.83-1031.
4. Yates, E.C.Jr., Wynne, E.C., Farmer, M.G. and Dermaries, R.N.: "Prediction of Transonic Flutter for a Supercritical Wing by Modified Strip Analysis," Journal of Aircraft, Vol.19, No.1, November 1982.
5. Garner, H.C.: "A Practical Framework for the Evaluation of Oscillating Aerodynamics Loading on Wings in Supercritical Flow," AGARD CP-226, April 1977.
6. Tijdeman, H.: "Investigation of the Transonic Flow around Oscillating Airfoils," NLR-TR-77090-U.
7. Isogai, K.: "Transonic Dip Mechanism of Flutter of a Swept Back Wing," Part II, AIAA Journal, Vol.19, No.9, September 1981.
8. Dowell, E.H., Bland, S.R. and Williams, M.H.: "Linear/Nonlinear Behavior in Unsteady Transonic Aerodynamics," AIAA Journal, Vol.21, No.1, January 1983.
9. Bland, S.R. and Edwards, J.W.: "Airfoil Shape and Thickness Effects on Transonic Airloads and Flutter," Journal of Aircraft, Vol.21, No.3, March 1984.
10. Guruswamy, P., and Goorjian, P.M.: "Comparisons Between Computations and Experimental Data in Unsteady Three-Dimensional Transonic Aerodynamics, Including Aeroelastic Applications," AIAA Paper No.82-0690.
11. Ricketts, R.H., Sandford, M.C., Siedel, D.A. and Watson, J.J.: "Transonic Pressure Distributions on a Rectangular Supercritical Wing Oscillating in Pitch," AIAA Paper No.83-0923.
12. Ashley, H.: "Role of Shocks in the 'Sub-Transonic' Flutter Phenomena," Journal of Aircraft, Vol.17, No.3, March 1980.
13. Nixon, D.: "On the Unsteady Transonic Shock Motions," AIAA Journal, Vol.17, No.10, October 1979.
14. Jameson, A., and Caughey, D.A.: "Numerical Calculation of the Transonic Flow Past a Swept Wing," NASA CR-153297, June 1977.
15. Ruhlin, C.L., Rauch, F.J.Jr. and Waters, C.: "Transonic Flutter Model Study of a Supercritical Wing and Winglet," Journal of Aircraft, Vol.20, No.8, August 1983.